

Supporting Information

Synthesis, structure, spectroscopic studies and magnetic properties of $\text{Cu}_2\text{N}_2\text{O}_4$ -, $\text{Cu}_2\text{N}_2\text{O}_2(\text{S}_2)$ -, $\text{Cu}_2\text{N}_2\text{S}_4$ -chromophores based on aminomethylene derivatives of pyrazole-5-one(thione)

Ali I. Uraev^a, Sergey E. Nefedov^b, Konstantin A. Lyssenko^c, Valery G. Vlasenko^d, Vladimir N. Ikorskii^e, Dmitrii A. Garnovskii^f, Nadezhda I. Makarova^a, Sergey I. Levchenkov^{f,g}, Igor N. Shcherbakov^g, Milica R. Milenkovic^h, Gennadii S. Borodkin^a

^a *Institute of Physical and Organic Chemistry of Southern Federal University, Stachki Ave. 194/2, Rostov-on-Don, Russian Federation*

^b *Kurnakov Institute of General and Inorganic Chemistry, Russian Academy of Sciences, Leninsky prosp. 31, 119991, Moscow, Russian Federation.*

^c *A.N. Nesmeyanov Institute of Organoelement Compounds of Russian Academy of Sciences, Vavilova 28, Moscow, Russian Federation.*

^d *Research Institute of Physics of Southern Federal University, Stachki Ave. 194, Rostov-on-Don, Russian Federation.*

^e *Institute "International Tomography Center," Siberian Branch, Russian Academy of Sciences, Institutskaya 3A, 630090, Novosibirsk, Russian Federation.*

^f *Southern Scientific Center of Russian Academy of Sciences, Chekhova str. 41, 344006 Rostov-on-Don, Russian Federation.*

^g *Department of Chemistry, Southern Federal University, 7, Zorge Str., Rostov-on-Don, 344090, Russian Federation*

^h *University of Belgrade, Faculty of Chemistry, Studentski trg 12-16, 11000 Belgrade, Serbia*

1. EPR spectra of the complexes **10-13**.

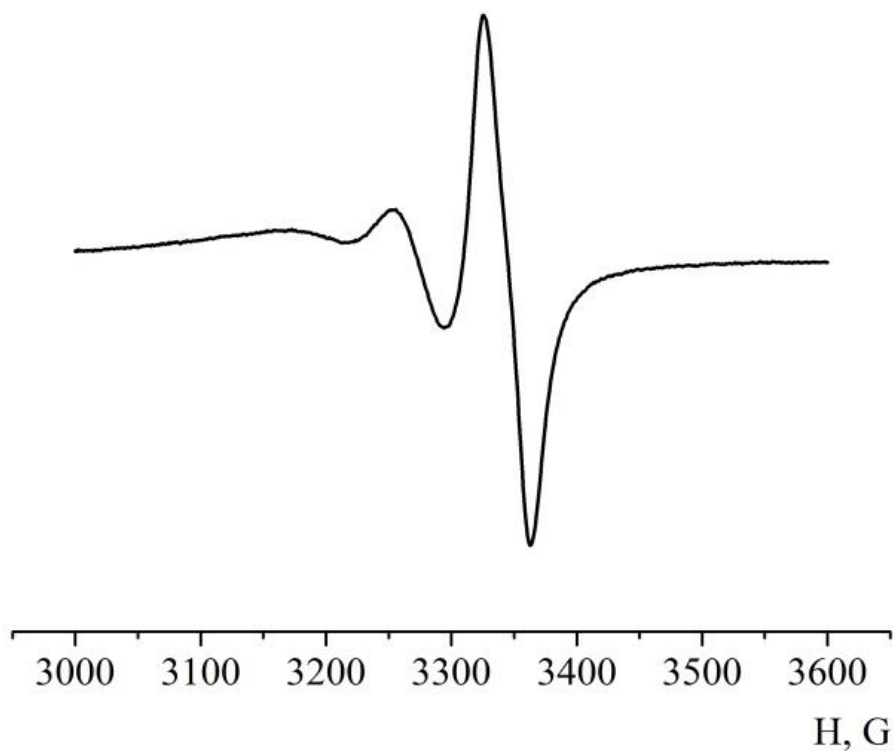


Fig. S1. Experimental ESR spectrum of complex **10** (DMSO, 290 K, $g = 2.13$, $a^{\text{Cu}} = 75$ G).

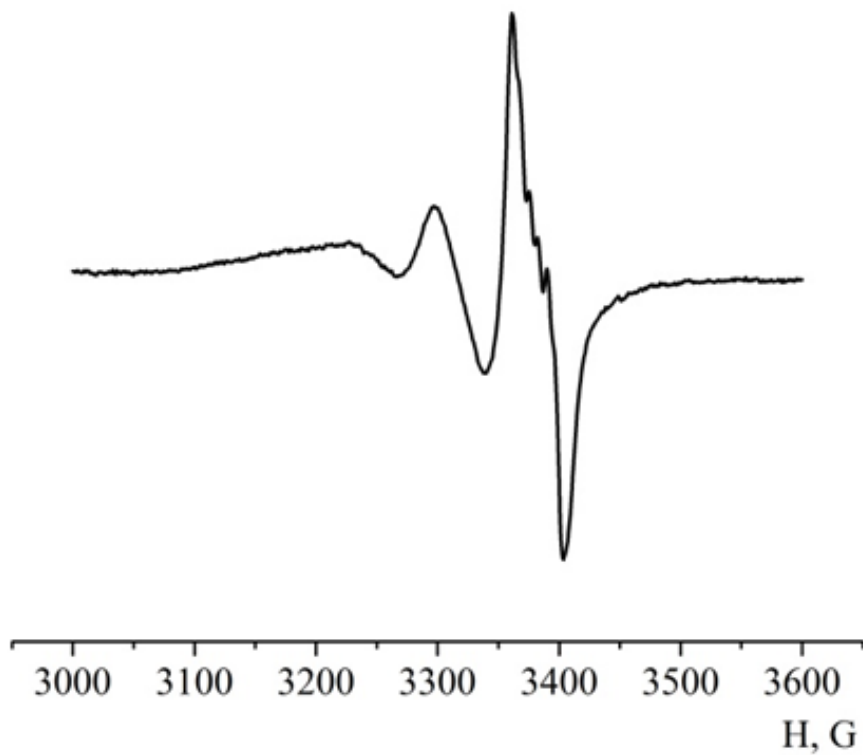


Fig. S2. Experimental ESR spectrum of complex **11** (DMSO, 290 K, $g = 2.10$, $a^{\text{Cu}} = 67$ G).

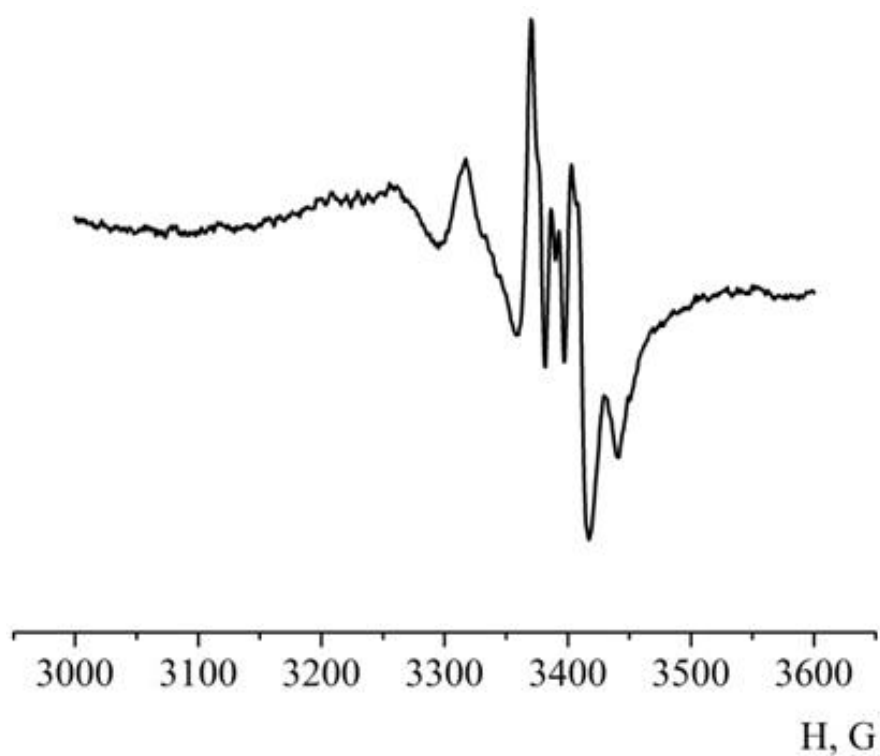


Fig. S3. Experimental ESR spectrum of complex **12** (DMSO, 290 K, $g = 2.08$, $a^{\text{Cu}} = 57$ G).

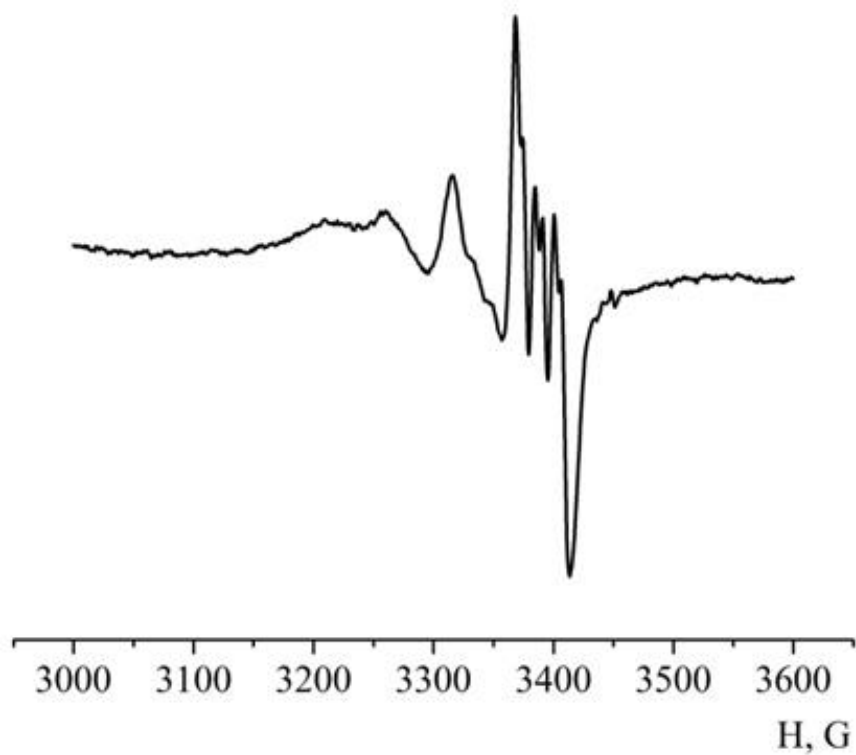


Fig. S4. Experimental ESR spectrum of complex **13** (DMSO, 290 K, $g = 2.08$, $a^{\text{Cu}} = 57$ G).

2. Molecular orbital description and electronic spectra

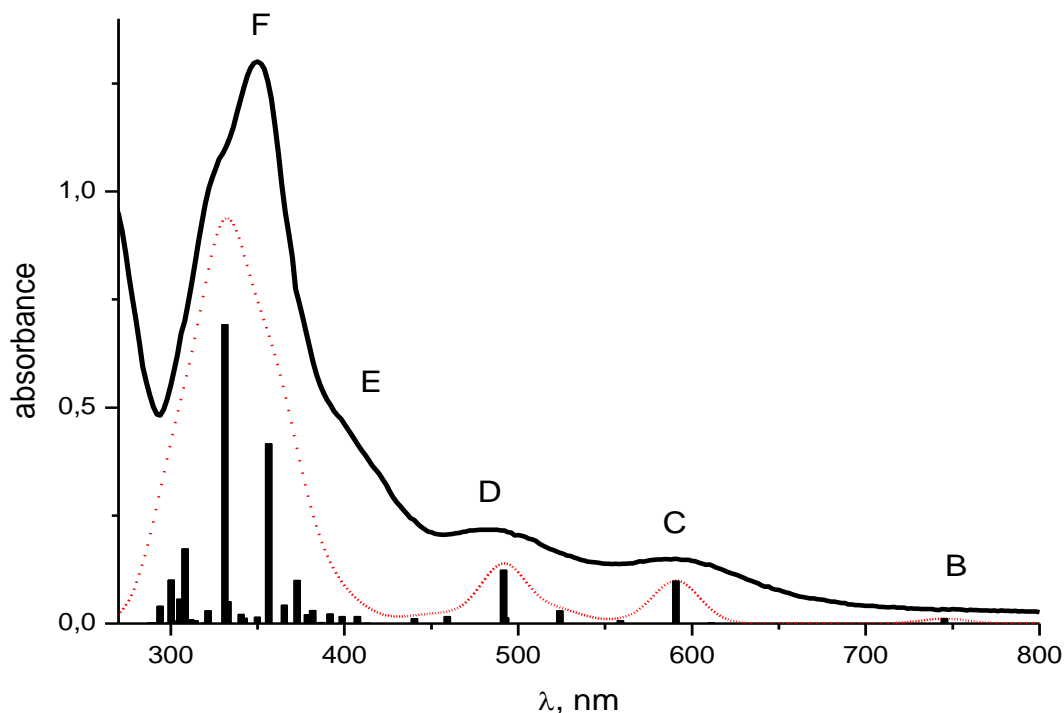


Fig. S5. The experimental (solid black line) and calculated (dash red line) electronic absorption spectra of complex **12** in CH_2Cl_2 solution. The vertical lines show the wavelengths of electronic transitions, the ordinates of lines of equal values of the oscillator strength of the corresponding electronic transitions.

Table S1. Calculated wavelengths (λ), energies (E), oscillator strengths (f), involved molecular orbitals and their contributions for different electronic transitions in complex **12** according to TD-DFT calculations.

λ_{cal} , nm	E, eV	Electronic transitions, (contribution, %)	f	Character
1078.13	1.150	HOMO \rightarrow LUMO (52%)	0.03	$\pi_{\text{L}} \rightarrow \pi_{\text{L}}^*$ LLCT
745.36	1.663	HOMO-2 \rightarrow LUMO (92%)	0.01	$\pi_{\text{L}} \rightarrow \text{d}$ LMCT $n_{\text{ter}}(\text{S}) \rightarrow n_{\text{br}}^*(\text{S})$
590.78	2.099	HOMO-3 \rightarrow LUMO (78%)	0.10	$\pi_{\text{L}} \rightarrow \text{d}$ LMCT $\pi_{\text{L}} \rightarrow n_{\text{br}}^*(\text{S})$

491.63	2.522	HOMO-6 \rightarrow LUMO (57%) HOMO-14 \rightarrow LUMO (11%)	0.12	$\pi_L \rightarrow d$ LMCT $\pi_L \rightarrow n^*_{br}(S)$
407.42	3.043	HOMO-22 \rightarrow LUMO (12%) HOMO-19 \rightarrow LUMO (14%) HOMO-14 \rightarrow LUMO (12%) HOMO-10 \rightarrow LUMO (14%)	0.02	$\pi_L \rightarrow d$ LMCT $\pi_L \rightarrow n^*_{br}(S)$
356.45	3.478	HOMO-4 \rightarrow LUMO+1 (56%)	0.42	$\pi_L \rightarrow n^*_{br}(S)$
331.21	3.743	HOMO-17 \rightarrow LUMO (20%) HOMO-14 \rightarrow LUMO (10%) HOMO-12 \rightarrow LUMO (19%)	0.69	$\pi_L \rightarrow d$ LMCT

Table S2. The energies and fragment compositions of MOs for complex **12**.

N	MO (α)	Energy, eV	Cu1	Cu26	S2 _{ter}	S27 _{ter}	S3 _{br}	S28 _{br}	L1	L2
175	HOMO-22	-8.272	0.18	0.3	0.03	0.04	0.03	0.04	0.15	0.23
176	HOMO-21	-8.182	0.19	0.18	0.03	0.03	0.01	-	0.27	0.27
177	HOMO-20	-8.171	0.33	0.33	0.02	0.03	0.01	0.02	0.13	0.13
178	HOMO-19	-8.082	0.22	0.14	0.05	0.04	0.04	0.05	0.27	0.2
179	HOMO-18	-8.071	0.2	0.25	0.04	0.05	0.01	0.01	0.18	0.25
180	HOMO-17	-8.007	0.22	0.24	0.03	0.03	0.04	0.04	0.19	0.21
181	HOMO-16	-7.919	0.2	0.2	0.05	0.05	0.03	0.03	0.22	0.21
182	HOMO-15	-7.738	0.4	0.31	0.03	0.02	0.01	0.02	0.11	0.1
183	HOMO-14	-7.715	0.2	0.33	0.01	0.02	0.04	0.03	0.17	0.19
184	HOMO-13	-7.443	0.37	0.37	0.04	0.04	-	-	0.09	0.09
185	HOMO-12	-7.253	0.15	0.16	0.1	0.1	0.09	0.08	0.17	0.17
186	HOMO-11	-7.079	0.11	0.11	0.05	0.06	0.06	0.06	0.26	0.28
187	HOMO-10	-7.051	-	0.01	0.03	0.04	-	-	0.39	0.5
188	HOMO-9	-7.035	0.09	0.09	0.04	0.03	-	0.01	0.41	0.31

189	HOMO-8	-6.955	0.03	0.03	0.02	0.02	0.02	0.03	0.43	0.42
190	HOMO-7	-6.906	0.05	0.05	0.07	0.07	0.04	0.04	0.34	0.34
191	HOMO-6	-6.594	0.10	0.13	0.03	0.03	0.06	0.1	0.22	0.33
192	HOMO-5	-6.588	0.12	0.1	0.01	-	0.16	0.12	0.29	0.18
193	HOMO-4	-6.113	0.06	0.06	0.02	-	0.02	-	0.42	0.43
194	HOMO-3	-6.021	0.05	0.05	0.07	0.06	0.03	0.03	0.36	0.35
195	HOMO-2	-5.780	0.03	0.02	0.24	0.13	-	-	0.34	0.23
196	HOMO-1	-5.758	0.05	0.06	0.16	0.27	-	-	0.17	0.28
197	HOMO	-5.021	0.18	0.18	0.07	0.07	0.13	0.13	0.12	0.12
198	LUMO	-3.355	0.19	0.19	0.05	0.05	0.15	0.15	0.11	0.11

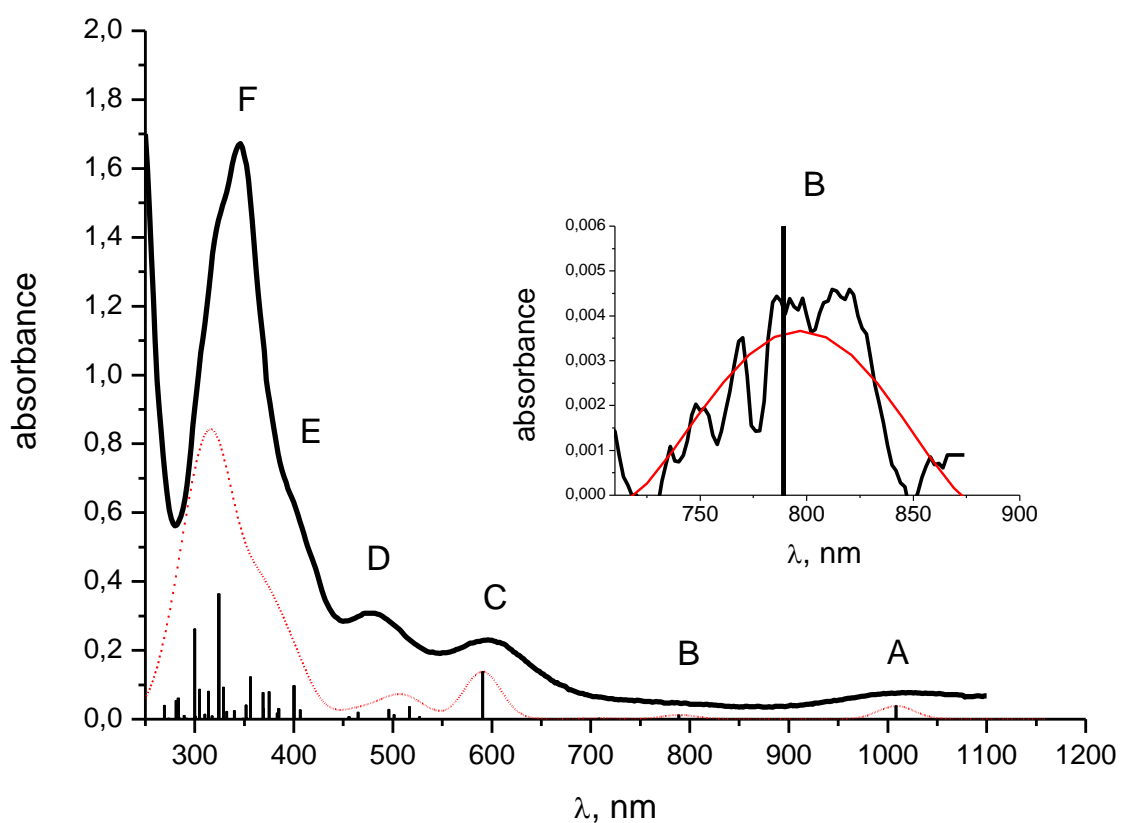


Fig. S6. The experimental (solid black line) and calculated (dash red line) electronic absorption spectra of complex **13** in CH_2Cl_2 solution. The vertical lines show the wavelengths of electronic transitions, the ordinates of lines of equal

values of the oscillator strength of the corresponding electronic transitions. The large-scale band *B* is shown in the inset.

Table S3. Calculated wavelengths (λ), energies (E), oscillator strengths (f), involved molecular orbitals and their contributions for different electronic transitions in complex **13** according to TD-DFT calculations.

λ_{cal} , nm	E, eV	Electronic transitions, (contribution, %)	f	Character
1008.34	1.230	HOMO \rightarrow LUMO (53%)	0.04	$\pi_{\text{L}} \rightarrow \pi_{\text{L}}^*$ LLCT
789.06	1.571	HOMO-2 \rightarrow LUMO (85%)	0.01	$\pi_{\text{L}} \rightarrow \text{d}$ LMCT $n_{\text{ter}}(\text{S}) \rightarrow n_{\text{br}}^*(\text{S})$
590.62	2.099	HOMO-3 \rightarrow LUMO (72%)	0.14	$\pi_{\text{L}} \rightarrow \text{d}$ LMCT $\pi_{\text{L}} \rightarrow n_{\text{br}}^*(\text{S})$
495.88	2.500	HOMO \rightarrow LUMO+2 (94%)	0.03	$\text{d} \rightarrow \pi_{\text{L}}^*$ MLCT $n_{\text{br}}(\text{S}) \rightarrow \pi_{\text{L}}^*$
400.18	3.098	HOMO-1 \rightarrow LUMO+1 (69%) HOMO-15 \rightarrow LUMO (10%)	0.10	LMCT $\pi_{\text{L}} \rightarrow \text{d}$ $\pi_{\text{L}} \rightarrow n_{\text{br}}^*(\text{S})$
375.11	3.305	HOMO-10 \rightarrow LUMO (42%) HOMO-2 \rightarrow LUMO+2 (35%)	0.08	$n_{\text{ter}}(\text{S}) \rightarrow \pi_{\text{L}}^*$ nLST
356.28	3.480	HOMO-4 \rightarrow LUMO+1 (51%) HOMO-3 \rightarrow LUMO+2 (18%)	0.12	$\text{d} \rightarrow \pi_{\text{L}}^*$ MLCT
324.15	3.825	HOMO-5 \rightarrow LUMO+1 (66%)	0.36	$n_{\text{br}}(\text{S}) \rightarrow \pi_{\text{L}}^*$ nLST

Table S4. The energies and fragment compositions of MOs for complex **13**.

N	MO (α)	Energy, eV	Cu1	Cu36	S2 _{ter}	S37 _{ter}	S3 _{br}	S38 _{br}	L1	L2
166	HOMO-15	-7.936	0.30	0.34	0.03	0.04	0.01	-	0.12	0.15
167	HOMO-14	-7.917	0.33	0.32	0.05	0.05	0.01	0.02	0.12	0.10

168	HOMO-13	-7.790	0.32	0.30	0.01	-	0.05	0.05	0.13	0.13
169	HOMO-12	-7.659	0.21	0.20	0.02	0.02	0.04	0.04	0.24	0.24
170	HOMO-11	-7.578	0.34	0.33	0.05	0.05	-	-	0.11	0.11
171	HOMO-10	-7.374	0.06	0.05	0.03	0.03	0.01	0.01	0.40	0.41
172	HOMO-9	-7.274	0.28	0.29	0.04	0.04	-	-	0.17	0.17
173	HOMO-8	-7.171	0.18	0.16	0.11	0.11	0.08	0.08	0.15	0.14
174	HOMO-7	-6.842	0.12	0.12	0.06	0.06	0.07	0.07	0.25	0.25
175	HOMO-6	-6.616	0.10	0.10	0.02	0.02	0.06	0.06	0.32	0.32
176	HOMO-5	-6.499	0.12	0.12	0.04	0.04	0.13	0.13	0.21	0.21
177	HOMO-4	-6.157	0.10	0.10	0.05	0.05	0.07	0.07	0.28	0.29
178	HOMO-3	-6.013	0.07	0.07	0.13	0.13	0.05	0.05	0.26	0.25
179	HOMO-2	-5.784	0.04	0.04	0.12	0.14	0.03	0.03	0.29	0.31
180	HOMO-1	-5.727	0.06	0.06	0.21	0.19	-	-	0.25	0.22
181	HOMO	-5.086	0.17	0.17	0.09	0.09	0.11	0.11	0.13	0.13
182	LUMO	-3.377	0.20	0.20	0.06	0.06	0.13	0.13	0.11	0.11
183	LUMO+1	-2.050	0.02	0.02	0.03	0.03	-	-	0.43	0.45
184	LUMO+2	-1.888	0.05	0.05	0.02	0.02	-	-	0.44	0.41